Cancer Letters 440–441 (2019) 168–179

Contents lists available at ScienceDirect

Cancer Letters

journal homepage: www.elsevier.com/locate/canlet

Original Articles

Primate-specific miR-944 activates p53-dependent tumor suppression in human colorectal cancers

Yoon-Jin Kim[a], Jeong Hwa Lee[a], Soll Jin[a], Jung Hoon Kim[b], Sang Hoon Kim[a,*]

[a] Department of Biology, Kyung Hee University, Seoul, 02447, Republic of Korea
[b] Department of Radiology, Seoul National University Hospital, Seoul, 03080, Republic of Korea

ARTICLE INFO

Keywords:
miR-944
p53
Tumor suppressor
Primate specific miRNA
Colorectal cancer

ABSTRACT

As cancers with a high incidence rate, colorectal cancers are a main cause of cancer-related death. MicroRNAs are often deregulated in cancers. The primate-specific miR-944, located in a p63 intron, is known to be highly expressed in patients exhibiting low colorectal cancer recurrence rates. However, the biological functions of miR-944 in colorectal cancers remain unclear. In this study, we found that miR-944 was downregulated in colorectal cancer tissues, and inhibited cancer cell growth in a xenograft mouse model. The overexpression of miR-944 caused G1 phase arrest and increased p53 expression in cancer cells. p53 stability was enhanced by miR-944s targeting E3 ligases COP1 and MDM2. Overexpression of COP1 and MDM2 restored cell growth inhibition caused by miR-944. Taken together, our results suggest that miR-944 acts as a potential tumor suppressor in colorectal cancers through the ubiquitin-proteasome system.

1. Introduction

Colorectal cancers are one of the most common cancers in the world. Although regular screening and development of diagnostic method improved early detection and treatment of cancers, colorectal cancers are known to display high recurrence rates after surgery and remain the third leading cause of cancer-related mortality [1]. The development of colorectal cancers occurs because of oncogene and tumor suppressor gene deregulation leading to the sequential progression from adenoma to carcinomas [2].

MicroRNAs (miRNAs) are small non-coding RNA regulating gene expression, and play roles in various biological events. Since deregulation of genes related to the processes of cell cycle, apoptosis, and senescence causes the development of cancers, miRNAs are implicated in carcinogenesis as gene regulators [3]. Additionally, over 50% of miRNA genes are located in cancer-associated genomic regions or in fragile sites. Many onco-miRNAs and tumor suppressor miRNAs have been found to be epigenetically altered in cancer [4]. In colorectal cancers, miRNAs are involved in tumor development from neoplasia to metastasis and angiogenesis. During colorectal cancer progression, inhibition of p53 function is the key step in the transition from adenoma to carcinoma. Since many genes are involved complicatedly in the p53 pathway, the miRNAs participating in p53 activation are not fully characterized.

Nearly 30% of miRNAs are conserved only in primates; primate-specific miRNAs are implicated in development, neuronal function and carcinogenesis. The primate-specific miRNAs, miR-637 and miR-4423, are downregulated in hepatocellular carcinoma and lung cancers respectively, and inhibit tumorigenesis as tumor suppressors [5,6]. MicroRNA-944 (miR-944) is another primate-specific miRNA, only expressed in great apes and the rhesus monkey. It is an intronic miRNA located within the p63 gene locus. The expression of miR-944 in cancer cells has been reported in several cancer miRNA-profiling studies. In colorectal cancer, miR-944 expression is epigenetically silenced [7]. In many cancers, including colorectal cancer, high expression of miR-944 is a good prognostic marker for both survival and relapse, and is associated with increased drug sensitivity [8–10]. The effect of miR-944 on malignant progression is poorly understood despite the availability of some related screening data in several cancer studies. According to our recent study, miR-944 increases p53 expression during the differentiation of skin keratinocytes [11]. Since the regulation of p53 expression is closely related to tumors, we have focused on the mechanism of the miR-944-mediated p53 activation in tumor cells. Herein, we demonstrate that miR-944 targets MDM2 and COP1, increasing p53 stability.

* Corresponding author. Department of Biology, Kyung Hee University, 26 Kyunghee-daero, Dongdaemun-gu, Seoul, 02447, Republic of Korea.
E-mail address: shkim@khu.ac.kr (S.H. Kim).

https://doi.org/10.1016/j.canlet.2018.10.029
Received 3 August 2017; Received in revised form 4 September 2018; Accepted 10 October 2018

2. Materials and methods

2.1. Cell culture and stable cell line construction

Colorectal cancer cell lines (HCT116, HCT116 $^{p53-/-}$, LoVo, RKO, HCT15, HT29, SW480, and SW620) and COS7 cells were incubated at 37 °C in a humidified chamber at 5% CO_2. HCT116 $^{p53-/-}$ cell was donated from HyunSook. Lee, Seoul National University, Republic of Korea. HCT116, HCT116 $^{p53-/-}$ and HT-29 cells were cultured in McCoy's 5a medium; RKO in MEM; LoVo in F12K medium, HCT-15, SW480 and SW620 in RPMI 1640 medium, and COS7 cells in DMEM. All media were supplemented with 10% FBS and 1% penicillin-streptomycin. Lipofectamine RNAiMAX (Invitrogen, Carlsbad, CA, USA) was used for RNA-oligonucleotide transfection, whereas plasmid and RNA-oligonucleotide co-transfections were performed using Lipofectamine 2000 (Invitrogen), according to the manufacturer's instructions. All oligonucleotides, including microRNA mimics, microRNA inhibitors and siRNAs were purchased from GenePharma (Shanghai, China). For establishment of a stable miR-944 expressing cell line, HCT116 cells were transfected with precursor miRNA expression constructs containing a puromycin resistance gene (Genecopoeia, Rockville, MD, USA) using Lipofectamine 2000 (Invitrogen). Cells were selected by incubation in medium containing 1 μg/mL puromycin (Sigma-Aldrich) for 48 h post-transfection. Following selection, cell clones were validated using RT-qPCR. The constructed stable cell lines were maintained in McCoy's 5a medium containing 0.1 μg/mL puromycin.

2.2. Plasmids

To generate 3′-UTR reporter constructs, fragments of the COP1 and MDM2 3′-UTR containing the putative miR-944 binding site were amplified from human genomic DNA by PCR. Each amplified fragment was cloned into pGL3-control vectors (Promega, Madison, WI, USA). Seed match sites were changed by site-directed mutagenesis using the Stratagene QuickChange kit (Agilent, Santa Clara, CA, USA) in accordance with the manufacturer's instructions. All plasmids were tested by restriction digestion and clone constructs were verified by sequencing. The corresponding primers are listed in Supplemental Table 1.

2.3. Cell viability and BrdU analysis

Cell viability was measured by the Dojindo Cell Counting Kit-8 (CCK-8) (Kumamoto, Japan) according to the manufacturer's instructions. In brief, cells were seeded on 96-well plates. After attachment, cells were treated according to each study's protocol. Next, diluted CCK-8 reagent was added to each well and incubated for 1 h. Absorbance was measured at a wavelength of 450 nm using a Vmax microplate spectrophotometer (Molecular Devices, Sunnyvale, CA, USA). For analysis of cell proliferation, the Cell Proliferation ELISA BrdU Colorimetric Assay Kit (Roche, Basel, Switzerland) was used following the manufacturer's instructions. In brief, HCT116 cells (1000 cells per well) were seeded on 96-well plates. Next days, cells were transfected with microRNA mimics. Forty-eight hours after transfection, cells were incubated with BrdU for 2 h at 37 °C, fixed, and denaturated. Next, cells were incubated with anti-BrdU-POD solution for 90 min and then washed with PBS. Substrate solution was added to each well, and absorbance was measured at a wavelength of 370 nm using a Synergy MX microplate reader (BioTek Instruments, Winooski, VT, USA). The wavelength of 492 nm was used as a reference.

2.4. Colony formation assay

About 1000 stably transfected cells were seeded per well onto 6-well plates and incubated for 10 days. Culture media were replenished every 3 days. The colonies were fixed using 3.7% formaldehyde for 10 min, stained with 0.1% (w/v) crystal violet in 10% ethanol for 10 min, and washed with distilled water. Colonies that contained more than 100 cells were counted. Each assay was performed in triplicate.

2.5. Total RNA extraction and real-time qPCR analysis

Total RNA was isolated using the TRIzol reagent (Invitrogen). Quantitative RT-PCR was used for determining the mRNA levels of each gene. First, cDNA was synthesized using the MMLV-reverse transcriptase (Takara Bio, Shiga, Japan) and oligo-dT primers (Invitrogen). The reverse transcription reaction mixture was incubated with the iQ SYBR Green supermix (BioRad, Hercules, CA, USA), followed by real-time amplification and quantitation in Rotor Gene Q thermocycler (Qiagen, Courtaboeuf, France) according to the manufacturer's protocol. The fluorescence threshold value was calculated using the Rotor Gene Q software (Qiagen). Data were processed with the comparative cycle threshold method and expressed as fold increase relative to the basal transcription level. The amount of target mRNA was normalized using the GAPDH mRNA levels as a reference. The corresponding primers are listed in Supplemental Table 2. For microRNA quantitative RT-PCR, total RNA was extracted from colorectal cancer cell lines and xenograft tumor tissues using TRIzol (Invitrogen). Total RNA derived from normal human colon tissues was purchased from Clontech Laboratories (Mountain View, CA, USA). Primers and probes for hsa-miR-944 (Assay ID: 002189) and U6 snRNA (used as an internal control; Assay ID: 001973) were purchased from Applied Biosystems (Thermo Fisher Scientific, Waltham, MA, USA). The Applied Biosystems TaqMan MicroRNA Reverse Transcription Kit (Thermo Fisher Scientific) was used to synthesize cDNA for the individual microRNAs. After reverse transcription (42 °C, 30 min) and an initial denaturation step (85 °C, 5 min), the cDNA was amplified for 40 cycles (denaturation: 95 °C for 15 s; annealing-extension: 60 °C for 60 s). The Rotor Gene Q system was used for both amplification and detection. Expression of miR-944 was calculated with the $2^{-\Delta\Delta}$Ct method, using U6 snRNA for normalization.

2.6. Western blot analysis

Cells were washed with cold PBS and lysed in ice-cold lysis buffer (50 mM Tris–HCl, 150 mM NaCl, 1% NP-40, 0.1% SDS, protease inhibitor cocktail, 50 mM NaF, and 0.2 M Na_3VO_4). Protein extracts were separated by SDS polyacrylamide gel electrophoresis and blotted onto a nitrocellulose membrane. Blocking was performed at room temperature for 1 h in TBS-Tween 20 (TBS-T) with 5% nonfat milk, followed by incubation with the primary antibodies diluted in TBS-T. After washing with TBS-T, the membrane was incubated with horseradish peroxidase-conjugated secondary antibodies. The protein bands were visualized using an enhanced chemiluminescence kit (Santa Cruz Biotechnology, Dallas, TX, USA). Primary antibodies against the following proteins were used: CCND, CCNE, CCNA, CCNB, CDK4, CDK2, p53, and MDM2 (Santa Cruz); p27, p21, and Rb (Merck Millipore, Billerica, MA, USA), and phospho-Rb (Ser 807/811); COP1 (Proteintech group, Rosemont, IL, USA), Pirh2 (Genetex, Irvine, CA, USA); β-Actin (Sigma-Aldrich). The intensity of protein bands was determined using Image J.

2.7. In vitro ubiquitination assay

RKO cells were co-transfected with 1 μg HA-Ubiquitin expression plasmid, 1 μg pCMV-p53, and 50 nM microRNA mimics (negative control or miR-944) for 48 h. Cells were treated with 10 μM MG132 for 6 h. The lysates were centrifuged for 10 min. Protein extracts were incubated with mouse anti-p53 antibody (Proteintech group) at 4 °C under constant agitation, and then immunoprecipitated with protein G agarose (Merck Millipore) at 4 °C for 2 h. Polyubiquitinated p53 was detected by western blotting using anti-HA antibody (MBL, Ottawa, IL, USA).

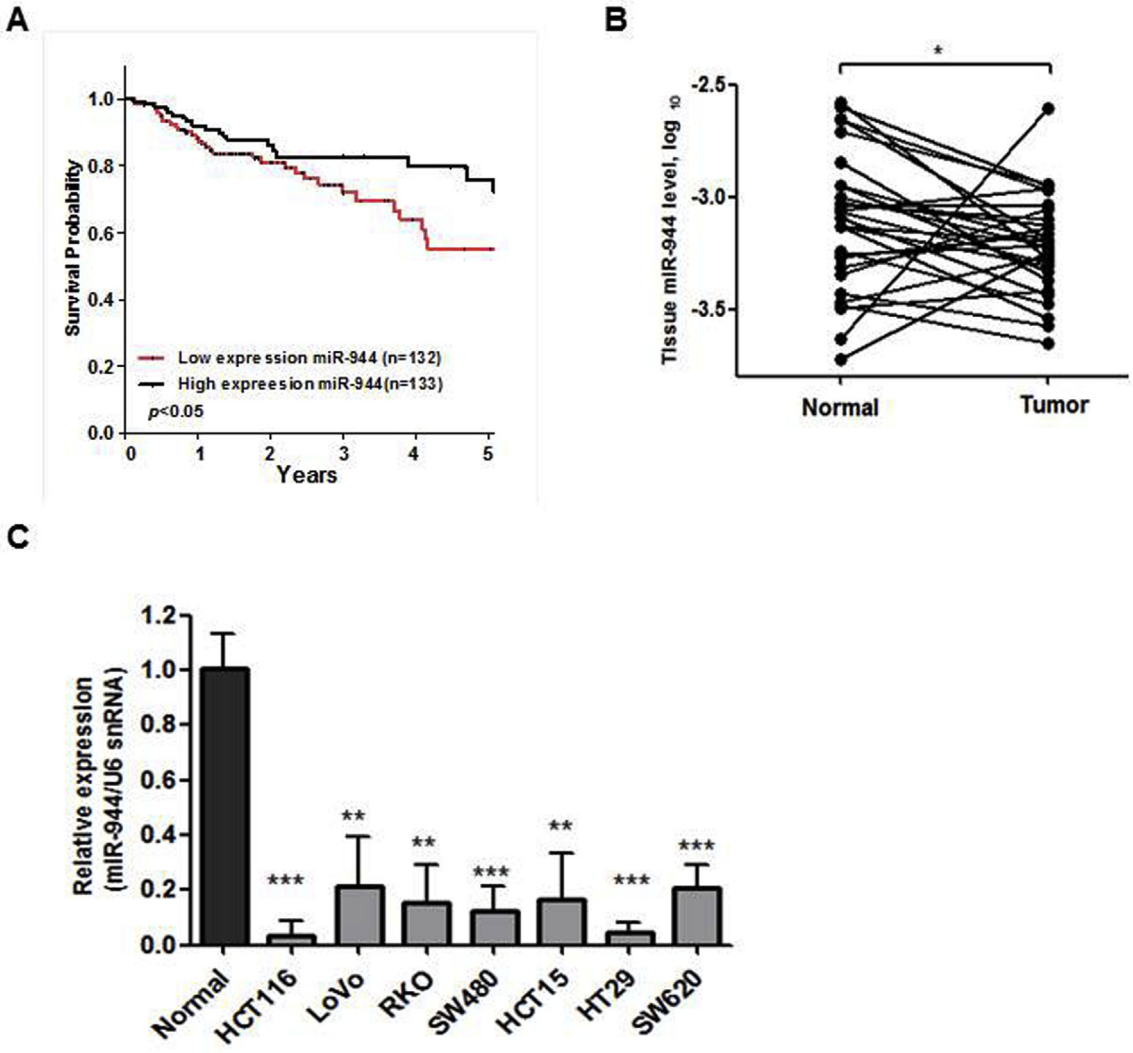

Fig. 1. miR-944 is down-regulated in publicly available GEO data set and cancer cell lines. (A) Kaplan-Meier survival curves display the overall survival rates of patients (data retrieved from TCGA) categorized by miR-944 expression levels. The Wilcoxon matched pair test was used to determine *P* values. (B) Analysis of miR-944 expression in colorectal cancer tissues. The miRNA array data for 31 colorectal cancer specimens were downloaded from the GEO database (GSE48267). The histogram display the expression values (expressed as long10 fold changes) of miR-944 in tumor tissues and paired adjacent normal tissues. $^{*}P < 0.05$. (C) RT-qPCR analysis of miR-944 expression levels in colorectal cancer cells and normal colon tissue. The expression value of miR-944 in normal tissue was arbitrarily set to 1. All data represent means ± SD. $^{**}P < 0.01$, $^{***}P < 0.001$.

2.8. Flow cytometry analysis

Cells were transfected with a miR-944 mimic and a negative scrambled control (GenePharma). At the indicated time points, cells were harvested, and fixed in 70% ethanol overnight. DNA staining was performed with a solution of 20 μg/mL propidium iodide containing 10 μg/mL RNase A. Approximately 2×10^4 cells were analyzed by flow cytometry using a Cytomics FC500 flow cytometer running on CXP software (Beckman Coulter, Mississauga, ON, Canada).

2.9. MicroRNA pull down assays

MicroRNA pull down assay were performed using a modified version of methods described by Orom et al. and Hayashida et al. [12,13]. Briefly, HCT116 cells were transfected with biotinylated (944-bio) or non-biotinylated (944-ss) miR-944 mimics. After 8 h, cells were harvested and cell lysates were incubated with streptavidin-agarose beads for 4 h at 4 °C. The beads were pre-blocked with RNase-free bovine serum albumin and yeast tRNA. After sedimentation by centrifugation, RNA was extracted with TRIzol (Invitrogen). For enrichment analysis of pulled down target genes, RNA was used to synthesize cDNA that was quantitated by RT-qPCR performed as described above. Values were normalized to input (cellular RNA not incubated with beads). The sequences of primers used in enrichment RT-PCR are provided in Supplementary Table 2.

2.10. Luciferase reporter assay

COP1 and MDM2 3' UTR reporter plasmids and miR-944 mimics were co-transfected into COS7 cells using Lipofectamine 2000 (Invitrogen). Forty-eight hours post-transfection, luciferase activities were measured; Renilla luciferase was used for normalization. All luciferase measurements were performed with the Dual Luciferase Assay kit (Promega) using a GloMax 20/20 luminometer (Turner Biosystems, Sunnyvale, CA, USA).

2.11. Tumor xenograft experiments

Four-week-old male BALB/c nude mice were purchased from Orient (Seongnam, Korea). The animals were maintained under specific

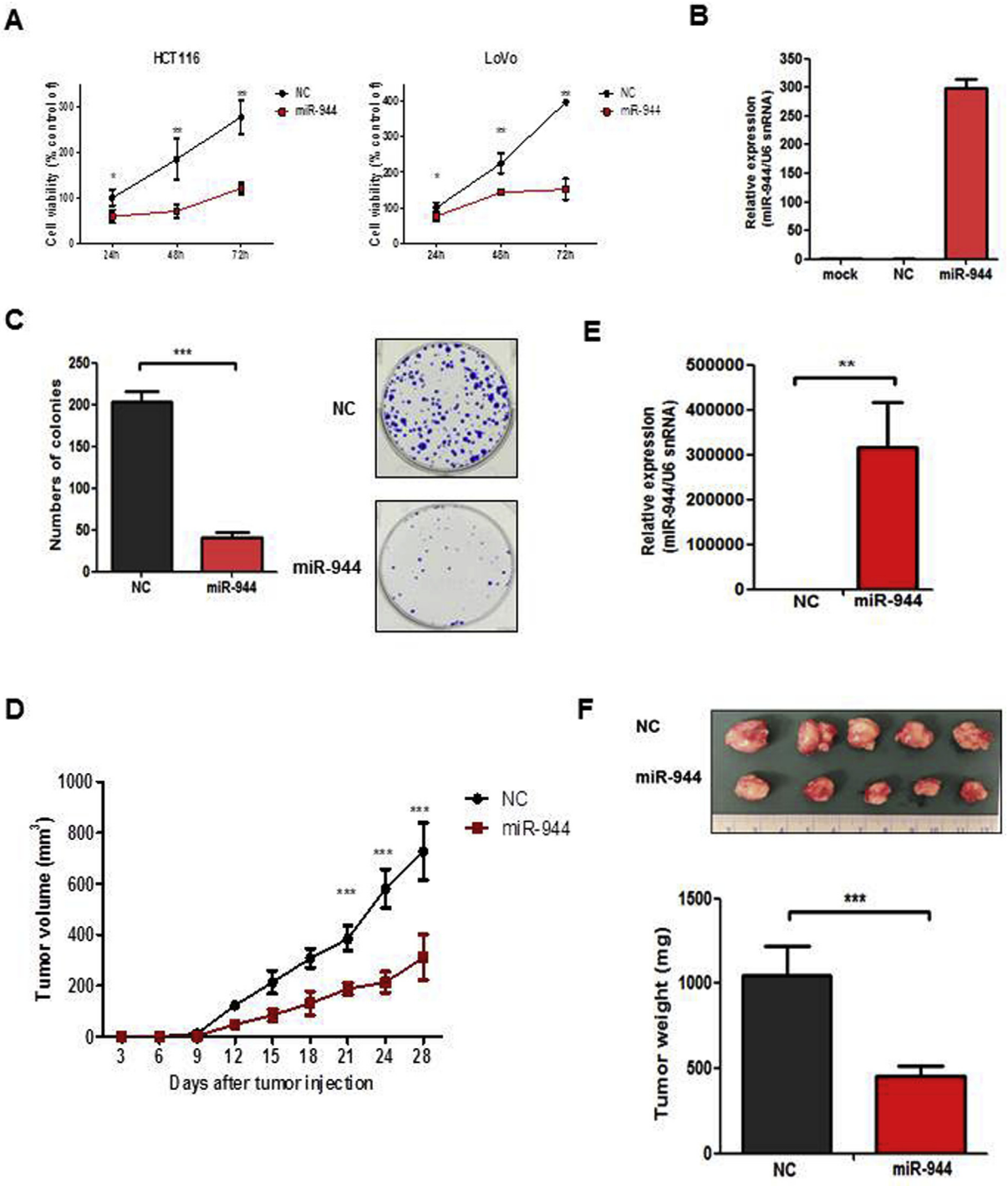

Fig. 2. Ectopic expression of miR-944 reduces the tumorigenic capacity of colorectal cancer cells. (A) HCT116 and LoVo cells were transfected with negative control oligonucleotide (NC) or a miR-944 mimic. Cell viability was determined using CCK8 assays at the indicated time points. Data are presented as means ± SD from three independent experiments. $^{*}P < 0.05$, $^{**}P < 0.01$. (B) Stably transfected miR-944 expressing cells were established and verified by RT-qPCR analysis. Mock indicates non-transfected cells and NC represents cells transfected with negative control oligonucleotides. (C) Colony formation assays were performed using NC or stably-transfected miR-944 expressing HCT116 cells. Relative colony numbers are displayed in the histogram at the left panel, whereas representative pictures are shown at the right panel. $^{***}P < 0.001$. (D) The effect of miR-944 on tumor formation in a nude mouse xenograft model. Stable HCT 116 cells overexpressing miR-944 or negative control miRNA (NC) were subcutaneously injected into the posterior right flank regions of nude mice (n = 5). The tumor size was measured every three days until day 28 post-injection. $^{***}P < 0.001$. (E) The expression of miR-944 from subcutaneous tumors in xenograft mice was analyzed by RT-qPCR. $^{**}P < 0.01$. (F) Xenograft tumors were removed at day 28 after tumor cell injection and weighed. $^{***}P < 0.001$. The photograph depicts removed tumors.

pathogen-free conditions at the Biomedical Research Institute of the Seoul National University Hospital. Stable HCT116 cells overexpressing miR-944 or control miRNA were subcutaneously injected (1×10^6 cells per injection) into the posterior flank of 6-week-old male BALB/c mice (five mice per group). Every 3 days until 28 days had passed, tumor volume was calculated as $0.5 \times W^2 \times L$, where L was the length (the largest diameter) and W was the width (the smallest diameter) of the tumor, both measured using a caliper. Animal experiments were

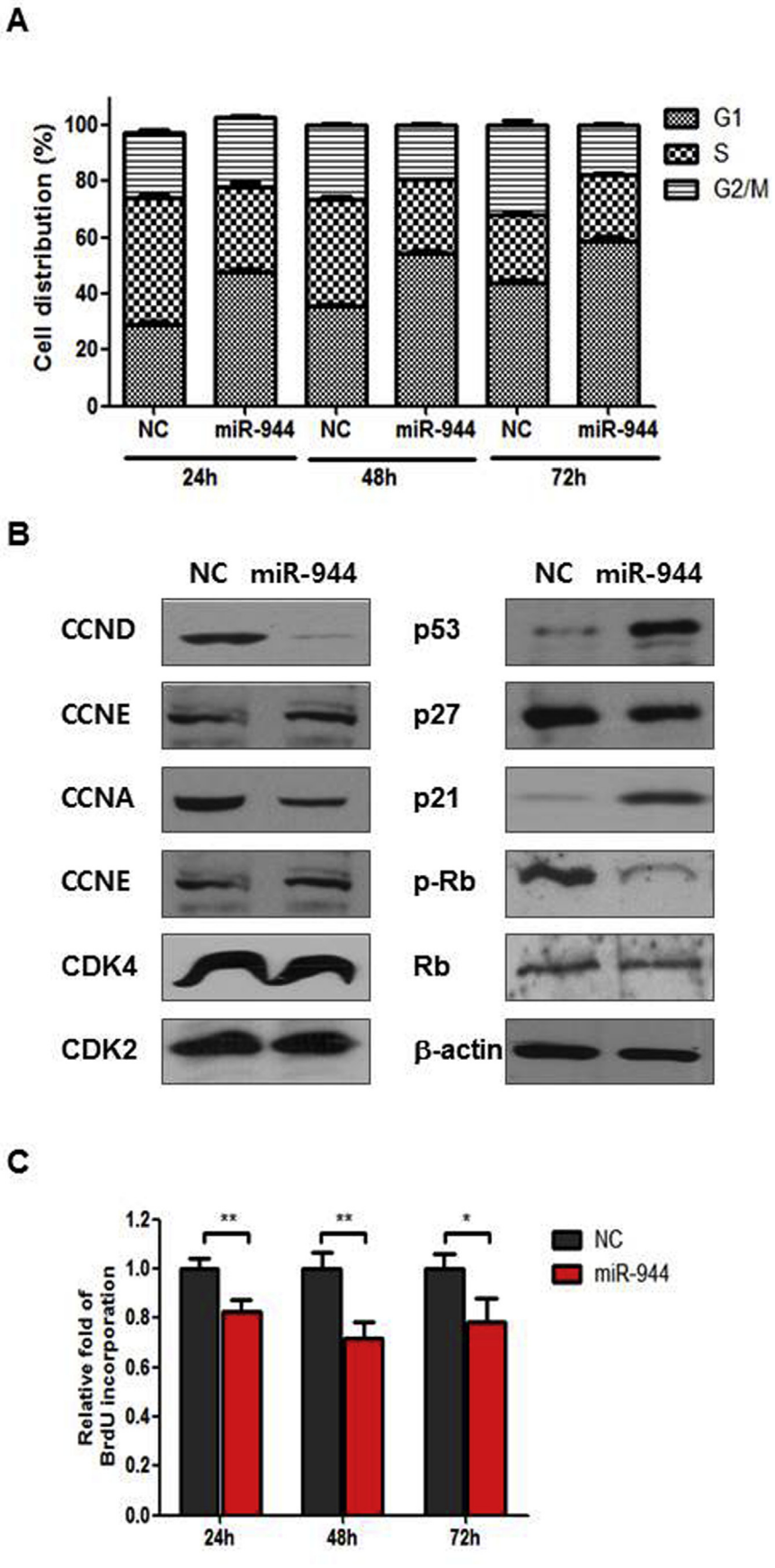

Fig. 3. miR-944 impedes cell cycle progression. (A) HCT116 cells were transfected with miR-944 mimic or negative control (NC) and harvested at the indicated time points. The cell cycle distributions were analyzed using propidium iodide staining and flow cytometry. Data were derived from at least three independent experiments and are presented as means ± SD. (B) Western blot analysis of the levels of endogenous cell-cycle regulator proteins in cells transfected with a miR-944 mimic or negative control. Representative data are shown. (C) The effect of miR-944 on cell proliferation. HCT116 cells were transfected with either a miR-944 mimic or a NC mimic and incubated for 24, 48 and 72 h. BrdU incorporation assay was then performed in each culture. $^{*}P < 0.05$, $^{**}P < 0.01$.

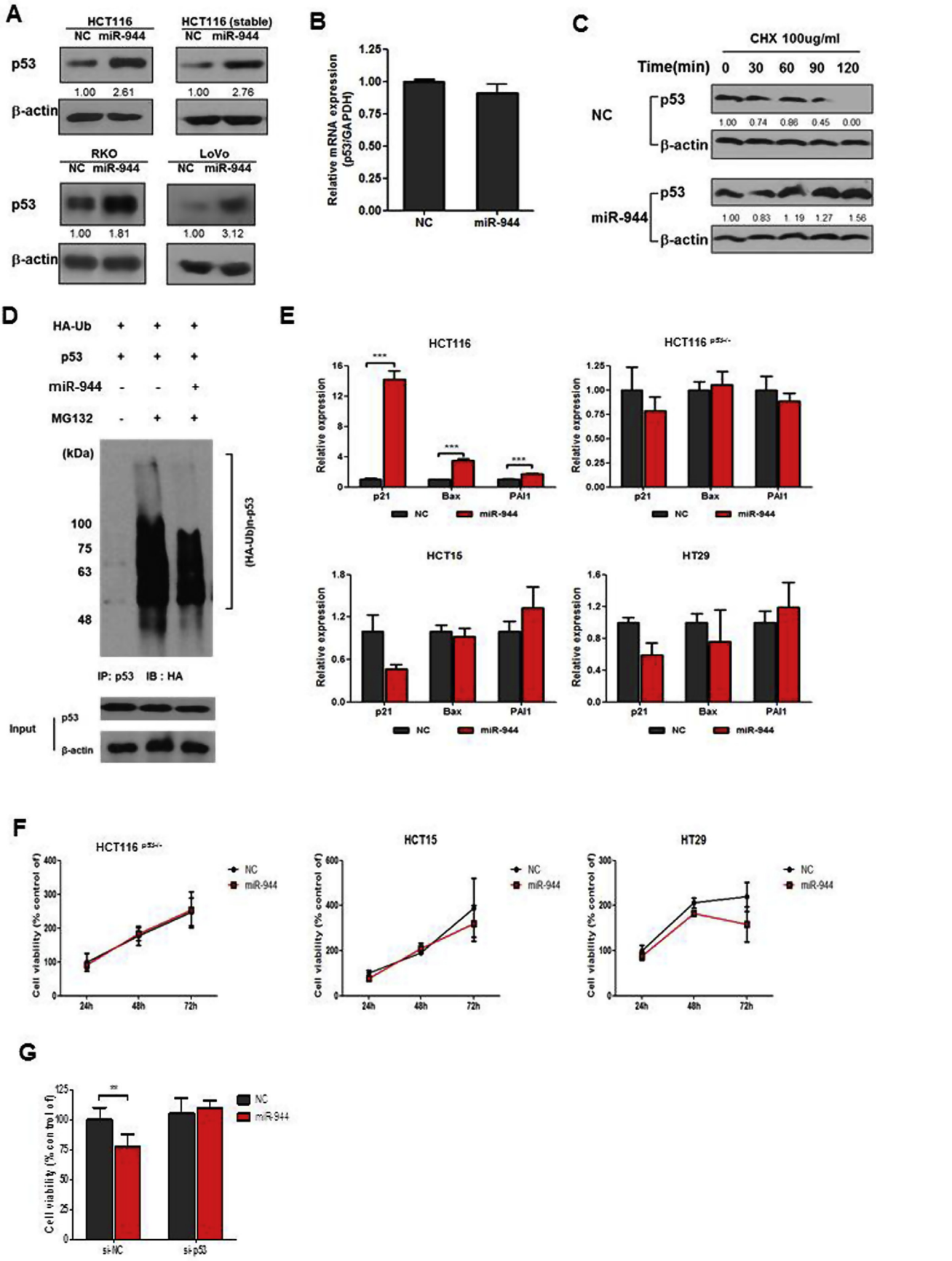

(caption on next page)

Fig. 4. miR-944 enhances p53 stability by inhibiting the ubiquitin/proteasome pathway. (A) Cell lysates were prepared from HCT116 cells stably expressing miR-944, as well as HCT116, RKO, and LoVo cells transfected with either a miR-944 mimic or a negative control (NC) mimic. Protein extracts were separated by SDS-PAGE and subjected to western blotting using an anti-p53 antibody. (B) The levels of p53 mRNA in the miR-944 transfected HCT116 cells were determined by RT-qPCR. (C) Cells were transfected with either miR-944 mimics or a NC mimic. At the indicated time points after cycloheximide (CHX) treatment, p53 protein levels were analyzed by western blotting. (D) Cells were co-transfected with a HA-tagged ubiquitin expression vector (HA-Ub), a p53 expression vector (p53), or microRNA mimics (miR-944 or NC) for 42 h. Cells were then treated with 10 μM MG132 or DMSO. Cell lysates either directly underwent SDS-PAGE and western blotting, or were first immunoprecipitated with anti-p53 antibody. The levels of p53 protein in input lysates are shown in the bottom panel. (E) HCT-116 (p53 wt), HCT116 ($p53^{-/-}$), HCT15, and HT29 cells were transfected with either miR-944 mimics or NC. The levels of p21, Bax, and PAI1 mRNAs were analyzed by RT-qPCR. Values were normalized to those of the NC group. ***$P < 0.001$. (F) HCT116 ($p53^{-/-}$), HCT15 and HT29 cells were transfected with either miR-944 mimic or NC. Cell viability was measured at the indicated time points. Data were normalized to time zero values. (G) HCT116 cells were cotransfected with microRNA mimics (miR-944 or NC), and siRNA against p53 (si-p53) or negative control siRNA (si-NC). Cell viability was assessed. **$P < 0.01$.

approved by the Institutional Animal Care and Use Committee (IACUC) of Seoul National University Hospital (IACUC approval No. 15-0194-S1A0) and performed according to its guidelines. Tumor weight was measured at the end of the experiment.

2.12. Data analysis

To analyze the expression of miR-944 in colon cancer patients, the Agilent Human miRNA Microarray data set GSE48267 was downloaded from NCBI GEO [14] and processed with the R statistical software. Differences in miR-944 levels between paired samples were evaluated with the Wilcoxon matched pairs test. Gene expression data from colorectal cancer were obtained from the GEO NCBI repository (GSE8671) [15]. Targetscan v5.2 and miRANDA were used to identify putative miRNA gene targets. Both clinical and microRNA sequencing data of Colon Adenocarcinoma (COAD) were downloaded from The Cancer Genome Atlas (TCGA) database. We queried the data for all COAD samples with level 3 microRNA expression data as well as with the accompanying clinical data. A total of 265 patients were selected for determination of the expression profiles of miR-944 and survival analysis.

2.13. Statistical analysis

All presented data were derived from at least three independent experiments and are shown as the mean ± S.D. The statistical significance of differences between groups was assessed using the Student's *t*-test. Kaplan-Meier analysis with log rank was applied for analyzing the survival of patients. Values of *P* (two-tailed tests) lower than 0.05 were considered statistically significant. Statistical calculations were performed using GraphPad Prism5 (GraphPad Sotfware, La Jolla, CA, USA).

3. Results

3.1. Suppression of miR-944 in cancer cell lines

MicroRNA profiling studies have reported miR-944 as a positive prognostic factor for survival and response to chemotherapy [7–10]. However, the specific role of miR-944 in colorectal cancers has not been evaluated. To assess the effect of miR-944 expression on clinical outcome, we determined the median values of miR-944 levels in colorectal cancer patients using data from The Cancer Genome Atlas (TCGA) portal. Kaplan-Meier analysis was performed, and the derived curves were used to compare the 5-year survival rates. Significantly higher mortality was observed in patients with low miR-944 expression (log-rank test, $P = 0.047$) than in those with high miR-944 expression (Fig. 1A). Next, we investigated the miR-944 expression pattern in tumor tissues and adjacent normal colorectal tissues derived from 31 colon cancer patients, using data from the Gene Expression Omnibus (GEO) database (GEO ID: GSE48267) [14]. The expression of miR-944 in tumor tissues was significantly lower than in adjacent normal tissues (Fig. 1B). In addition, we found that miR-944 expression in colorectal cancer cell lines was lower than that in normal colon tissues (Fig. 1C). These results consist with recently publicly data showing the down-regulated miR-944 expression in colorectal cancer [16]. Overall, miR-944 could be a potentially good marker for cancer diagnosis.

3.2. Reduction of cell viability by miR-944 in cancer cells

To examine the effects of miR-944 on cancer cell growth, the viability of HCT116 and LoVo colorectal cancer cells transfected with a miR-944 mimic was analyzed by the cell counting kit-8 (CCK-8) assay. Overexpression of miR-944 significantly attenuated cell growth in both HCT116 and LoVo cells (Fig. 2A). We also examined the effects of anti-miR-944 in cells expressing miR-944 mimic. Overexpression of miR-944 inhibitor increased cell viability in HCT116 cell expressing miR-944 mimic (Supplement Fig. 1). Since tumor cells are resistant to contact inhibition, we first established a HCT116 stable clone expressing pre-miR-944 to determine how miR-944 affects the colony forming ability of cells (Fig. 2B). The colony production capacity of cells over-expressing miR-944 was significantly reduced by 80% compared to control cells (Fig. 2C). Next, we investigated the anti-tumorigenic effect of miR-944 *in vivo* by using a xenograft mouse model. Stably transfected miR-944 or NC-miRNA expressing cells were subcutaneously injected into nude mouse and the mice were observed for 4 weeks. The first tumor in mice injected with miR-944 expressing cells was detected on the ninth day after cell injection. Mice injected with miR-944 expressing cells had smaller tumors compared to those injected with the NC-miRNA cells (Fig. 2D); the overexpression of miR-944 resulted in a significant reduction of 36–49% in tumor growth rate compared to the negative controls. The expression level of miR-944 in tumor tissues derived from injected mice was examined by qRT-PCR. Results showed that tumor xenografts from mice injected with miR-944 expressing cells had high levels of this miRNA, indicating that the high levels of miR-944 expression were retained during tumorigenesis (Fig. 2E). Four weeks after injection, xenograft tumors were removed and weighed. Tumors from mice that had been injected with miR-944 expressing stably transfected cells weighted 65% less than the control group (Fig. 2F). These results demonstrate that miR-944 suppresses tumorigenesis of colorectal cancer both *in vitro* and *in vivo*.

3.3. Suppression of cell cycle progress in miR-944 transfected cells

We analyzed the cell cycle distribution in cells transfected with a miR-944 mimic. As shown in Fig. 3A, miR-944 overexpression caused significant G1 phase-arrest in HCT116 cells in a time-dependent manner. To evaluate the cell cycle progress in cells expressing miR-944, the expression levels of cyclins (CCND, CCNE, CCNA and CCNB), CDKs (CDK4 and CDK2), and other cell cycle regulators (p53, p21, p27 and Rb) were analyzed. The expression of the G1 cyclin, CCND, was downregulated in cells transfected with miR-944 compared to the control (Fig. 3B). The overexpression of miR-944 increased p53 and p21 expression, whereas it reduced the levels of phosphorylated Rb. In addition, the number of cells displaying bromodeoxyuridine (BrdU) incorporation was lower in miR-944 transfectants than control cells, indicating a repression of DNA synthesis during the S phase in the miR-944 transfected HCT116 cells (Fig. 3C).

A

	miR-944 putative site
hsa-miR-944	3′ gaGUAGGCUACAUGUUAUUAAa 5′
COP1 3′UTR	272: 5′ uuCUUUUGAAUAAAAAUAAAUa 3′
hsa-miR-944	3′ gaguaGGCUACAUGUUAUUAAa 5′
MDM2 3′UTR	207: 5′ aacucCUAAUUUUAAAUAAUUu
hsa-miR-944	3′ gaguaggcUACAU--GUUAUUAAa 5′
Pirh2 3′UTR	3261: 5′ uuauuaaaAUUUAAUUGAUAAUUg 3′
hsa-miR-944	3′ gaGUAGGCUAC-AUGUUAUUAAa 5′
RNF2 3′UTR	1159: 5′ agCCUUCAAAGAAAAAAUAAUUu 5′
hsa-miR-944	3′ gagUAGGCUACA--UGUUAUUAAa 5′
Wip1 3′UTR	1888: 5′ guaAUCCUUUGUGAAAUAUAAUUc
hsa-miR-944	3′ gaguAGGCUACAUGUUAUUAAa 5′
Mule 3′UTR	516: 5′ uauuUCUGAUUU--CAUAAUUc 3′

B

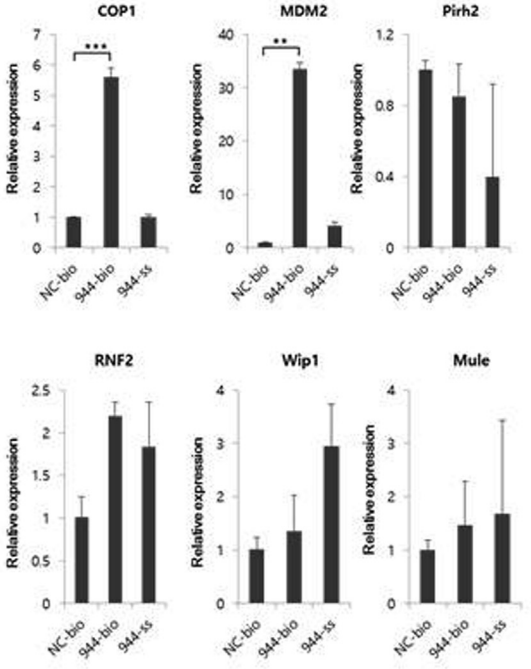

C

```
hsa-miR-944              3' gaGUAGGCUACAUGUUAUUAAa 5'
                              | |::|| | ||||| |
COP1 3'UTR (wt)    272:5' uuCUUUUGAAUAAAAAUAAAUa 3'
COP1 3'UTR (mut)        5' uuCUUUUGAAUAAAAAcgcAUa 3'

hsa-miR-944              3' gaguAGGCUACAUGUUAUUAAa 5'
                              |: || | |||||||
MDM2 3' UTR (wt)   207:5' aacucCUAAUUUUAAAUAAUUu 3'
MDM2 3' UTR (mut)       5' aacucCUAAUUUUAcAUAcgUu 3'
```

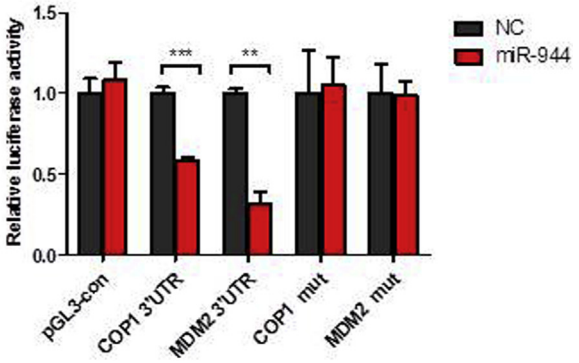

D

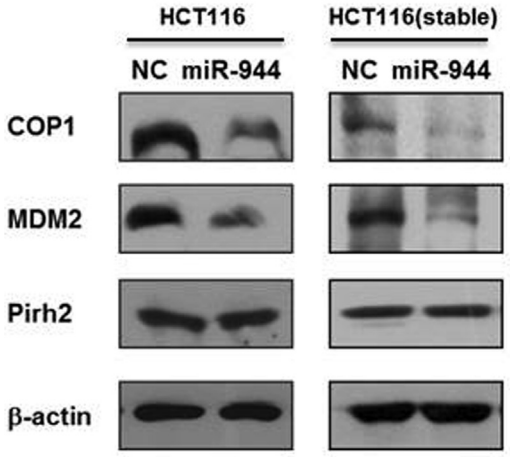

E

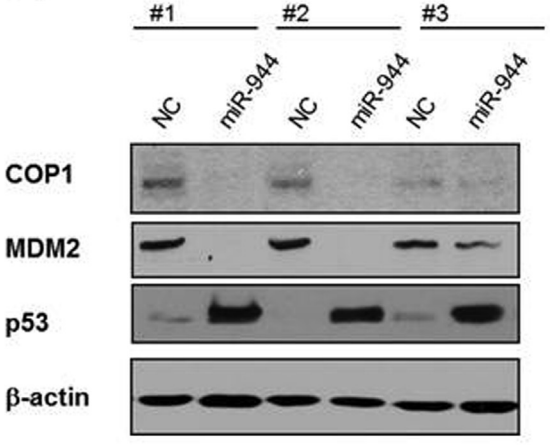

(caption on next page)

Fig. 5. COP1 and MDM2 are direct targets of miR-944. (A) Putative miR-944 target sites within the 3′-UTRs of p53-negative regulators as predicted by the TargetScan and miRanda algorithms. (B) HCT116 cells were transfected with biotinylated miR-944 mimic (944-bio), biotinylated negative control (NC-bio), or non-biotinylated single strand miR-944 mimic (944-ss). At 8 h post-transfection, RNA pull-down assays were performed by using streptavidin agarose beads, followed by RT-qPCR to measure fold enrichment of target genes. $^{**}P < 0.01$, $^{***}P < 0.001$. (C) COP1 or MDM2 3′-UTRs containing putative wild type (wt) or mutant type (mut) miR-944 binding sites were cloned into luciferase expression pGL3-control vectors. The mutated nucleotides are written in lower-case italics. COS-7 cells were co-transfected with the indicated luciferase vectors (pGL3-con: pGL3-control; COP1 3′UTR: pGL3-containing wild-type COP1 3′-UTR; MDM2 3′UTR: pGL3-containing wild-type MDM2 3′-UTR; COP1 mut: pGL3-containing mutant COP1 3′-UTR; MDM2 mut: pGL3-containing mutant MDM2 3′-UTR) together with miRNA mimics (miR-944 or NC). Luciferase activity was measured and normalized to that of the NC transfected cells. Each experiment was conducted at least three independent times. Data are presented as means ± SD. $^{**}P < 0.01$, $^{***}P < 0.001$. (D) Cells were transfected with miR-944 mimic or NC. The levels of COP1, MDM2 and Pirh2 proteins were analyzed by western blotting. (E) Levels of p53, COP1 and MDM2 in transplanted tumors. Proteins of xenograft tumors were obtained from three representative sets. Expression levels of COP1, MDM2, and p53 were determined by western blot analysis.

3.4. Enhanced p53 stability in response to miR-944

Our previous study demonstrated that miR-944 upregulates p53 expression in keratinocytes [11]. This led us to hypothesize that miR-944 suppresses colorectal cancer cell growth by regulating p53 signaling. To test this hypothesis, we examined the effect of miR-944 on p53 expression in colorectal cancer cells. As shown in Fig. 4A, p53 protein levels were increased in cells transfected with a miR-944 mimic compared to those transfected with negative control oligonucleotides. Next, we investigated whether miR-944 regulates p53 level at the level of transcription. Contrary to protein levels, there was no significant difference in the p53 mRNA levels between the miR-944 transfected and the control cells (Fig. 4B), suggesting that the regulation of p53 by miR-944 occurs at a post-transcriptional level. In order to examine whether the stability of the p53 protein was altered by miR-944, we analyzed the half-life of p53 after treating miR-944 transfected HCT116 cells with the protein synthesis inhibitor, cycloheximide. As shown in Fig. 4C, the levels of p53 in the negative control cells were rapidly decreased, whereas its presence was substantially sustained in the miR-944 overexpressing cells, indicating that miR-944 overexpression increases p53 half-life. We also examined whether the miR-944-induced increase in p53 stability is mediated through the regulation of proteasome. We found that ubiquitinated p53 was accumulated in the control cells after MG132 treatment, but this pattern attenuated in miR-944 overexpressed cells (Fig. 4D). Taken together, our data indicated that miR-944 enhanced the stability of p53 protein by inhibiting the ubiquitin proteasome system.

Meta-analysis of data derived from colorectal cancer studies revealed that the transactivity of p53 protein is reduced; thus, the recovery of p53 transactivity in tumor cells is important for improving the efficiency of chemotherapy [17]. In order to find out if miR-944 can activate p53 signaling, we investigated the expression of p53-downstream genes. After overexpressing miR-944 in HCT116 cells, we examined the expression of the cell cycle-related p53 target gene p21, the apoptosis-related gene Bax, and the senescence-related gene PAI1. Results showed that miR-944 increased the expression of p21, Bax, and PAIl in p53-wild type HCT116 cells, whereas the expression of these genes was not altered in p53-null HCT116 cells (HCT116 $^{p53-/-}$) and p53-mutant colorectal cancer cell lines (HT-15 and HCT-29) (Fig. 4E), signifying that miR-944 not only increases the expression levels of p53, but also enhances transactivation in the p53 signaling pathway. In addition, we examined the viability of p53-null and p53-mutant cells overexpressing a miR-944 mimic; we observed that miR-944 did not lead to growth inhibition in these cells (Fig. 4F). Similar results were acquired from cells whose p53 expression had been knocked down using p53-specific siRNA, i.e., the miR-944 mimic did not affect their viability (Fig. 4G). Additionally, we examined the cell viability in HCT116 p53 null cells transfected with control, p53 wild-type or p53 mutant (R249S) vectors, respectively. We observed that miR-944 attenuate cell viability in the cells transfected with p53 wild-type vector, but not with control or p53 mutant (R249S) vector (Supplement Fig. 2). Taken together, these results indicate that miR-944 can stimulate p53-mediated signaling by increasing p53 stability.

3.5. Ubiquitin ligases COP1 and MDM2 are targeted by miR-944

We were interested in determining the miR-944 target genes that controlled p53 stability. In order to identify miR-944 target genes participating in the p53 pathway, we performed *in silico* analyses using TargetScan and miRANDA programs; we selected six candidate genes (COP1, MDM2, Pirh2, RNF2, Wip1, and Mule) that encode p53 negative regulators, and also have miR-944 seed regions in their 3′-UTRs (Fig. 5A). To confirm the association of miR-944 with these putative target genes, miRNA pull-down assays were conducted in HCT116 cells transfected with a biotinylated miR-944 mimic. Among the six candidate genes, the E3 ligase-encoding MDM2 and COP1 were found to be significantly associated with miR-944 in HCT116 cells (Fig. 5B). Luciferase reporter assays were performed to verify whether COP1 and MDM2 are directly regulated by miR-944. The overexpression of miR-944 significantly reduced the luciferase activity of the COP1 and MDM2 3′-UTR reporter constructs, whereas it did not affect the luciferase activity of COP1 and MDM2 3′-UTR mutant constructs (Fig. 5C). Furthermore, miR-944 overexpression reduced the levels of the MDM2 and COP1 proteins, but not Pirh2 (Fig. 5D). In tumors derived from the xenograft mouse model for miR-944, we confirmed that the expression of COP1 and MDM2 proteins was reduced compared to that in the negative control group (Fig. 5E). Taken together, these results indicate that COP1 and MDM2 are direct target genes of miR-944.

3.6. The anti-proliferative effect of miR-944 is mediated by COP1 and MDM2

We performed knockdown and functional restoration experiments to confirm that MDM2 and COP1 are functional targets of miR-944 in colorectal cancer cells. MDM2 and COP1 in HCT116 cells were knocked down using si-MDM2 and si-COP1, respectively (Fig. 6A). For si-MDM2, three different siRNAs against MDM2 were designed (Supplementary Table 3) and we found #3 si-MDM2 only work in the cells. So we used further study with #3 primer of si-MDM2. Unlike the negative controls, both the MDM2-and COP1-knocked down cells exhibited an inhibition of proliferation reminiscent of the phenotype observed in the miR-944 overexpressing HCT116 cells (Fig. 6B). For the functional restoration studies, HCT116 cells were transfected with a miR-944 mimic followed by co-transfection with 3′-UTR lacking expression vectors of human MDM2 or COP1. Western blot analysis was used to verify the restoration of MDM2 and COP1 expression in the respective cells (Fig. 6C). As shown in Fig. 6D, the restoration of the target gene expression abolished the anti-proliferative effect of the miR-944 mimic. In addition, we found that the colony formation ability, which had been inhibited by miR-944, recovered in the miR-944 expressing stably transfected cells after transfection with either a COP1 or a MDM2 expression vector lacking their 3′-UTR (Fig. 6E). These results suggest that COP1 and MDM2 are functional targets of miR-944 mediating its anti-proliferative effect in colorectal cancers.

4. Discussion

In the present study, we demonstrated that miR-944 inhibits cell

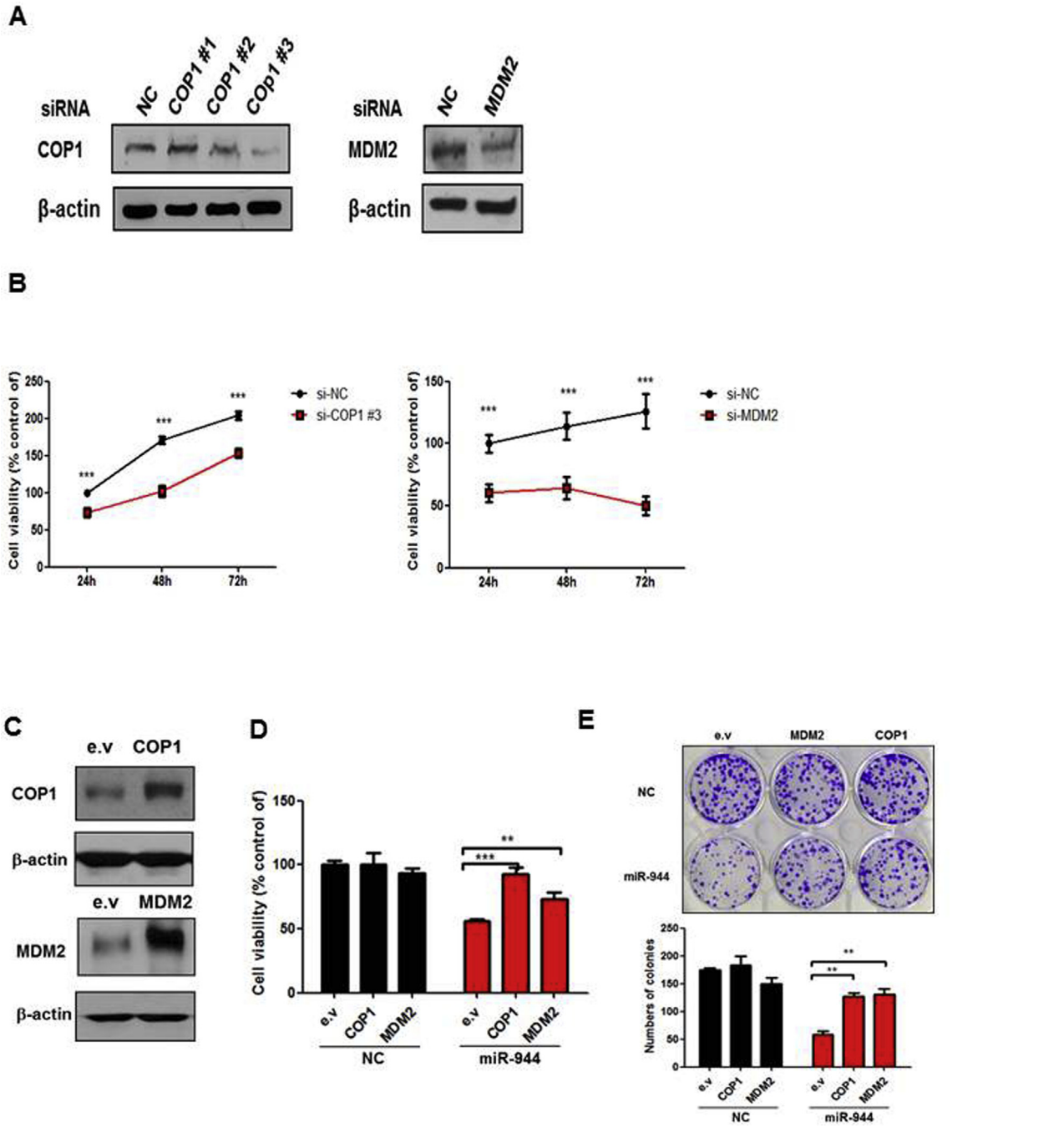

Fig. 6. COP1 and MDM2 are functional targets of miR-944 mediating its anti-proliferative effect. (A) Expression of COP1 and MDM2 was analyzed by western blotting in cells transfected with si-COP1, si-MDM2, or si-negative control (si-NC). For si-MDM2 primer design, three difference regions of MDM2 were selected. (B) Cells were transfected with si-COP1, si-MDM2, or si-NC. Cell viability was evaluated. $^{***}P < 0.001$. (C) Expression of COP1 or MDM2 was detected in cells by western blotting. e.v: empty vector. (D) HCT116 cells were co-transfected with both miRNA mimics (miR-944 or NC) and either a COP1 or a MDM2 expression vector lacking the respective 3′-UTR. Cell viability was evaluated. $^{**}P < 0.01$, $^{***}P < 0.001$. (E) Stable cells expressing miR-944 were transfected with either a COP1 or a MDM2 expression vector, and subjected to a colony formation assay. Colony numbers are displayed in the histogram at the bottom panel, whereas representative pictures are shown at the top panel. Data are expressed as means ± SD of triplicate experiments. $^{**}P < 0.01$, $^{***}P < 0.001$.

growth and induces p53-dependent cell death. P53 is a tumor suppressor that is regulated by miRNAs. Some oncogenic miRNAs directly target p53, whereas certain tumor-suppressive miRNAs target negative regulators of p53 such as the E3 ligase, MDM2. Several MDM2-targeting miRNAs are known, such as miR-192/194, miR-215, miR-143/145, miR-339-5p, and miR-661 [18–21]. MDM2 is just one of the E3 ligases that affect p53 stability; thus, miRNAs targeting only MDM2 are not sufficient to maintain p53 stability in cells. In our study, miR-944 was found to regulate p53 stability by independently targeting two E3 ligases, MDM2 and COP1. Double knock-down of these genes results in a synergistic increase in p53 stability [22]. Thus, miR-944 regulates p53 stability more efficiently than miRNAs targeting MDM2 alone.

Little is known about the regulatory mechanisms underlying COP1 expression, despite it being a critical regulator of p53 stability. DNA damage leads to the suppression of COP1 expression, stabilizing p53 [22,23]. COP1 is phosphorylated at the s387 residue by a DNA damage sensor kinase, ATM; this phosphorylation induces the self-degradation of COP1 through interaction with CSN6 and 14-3-3 delta. However,

ionizing radiation can also decrease COP1 expression in ATM-deficient cells [23], which implies the existence of other factors regulating COP1 expression. Since the levels of COP1 mRNA are not affected by DNA damage, post-transcriptional processes involving miRNAs must be critical for determining COP1 stability. However, a human COP1-targeting miRNA has not been reported yet. In the present study, the induction of miR-944 reduced the COP1 protein level. Thus, miR-944 is a regulator of COP1 expression in cells.

Although in the present study miR-944 exhibited a tumor-suppressive role in colorectal cancer cells, other studies have reported miR-944 as an oncogenic gene [24–26]. In cervical cancer, miR-944 does not affect cell cycle and apoptosis, but stimulates migration and invasion [24]. With respect to non-small cell lung cancer, the expression of miR-944 is dependent on cell type, with expression being higher in squamous carcinomas than in adenocarcinomas. Cells derived from squamous carcinomas stimulate invasion by overexpressing miR-944 [25]. However, the cancer cells used in these studies harbor abnormal p53 genotypes, such as p53 inactivation (HeLa, CaSki), p53 null (Calu-1), and p53 mutant (Sk-mes-1). One of the findings from the present study was that transfection of p53-mutant and p53-null colon cancer cells with a miR-944 mimic did not result in cell-growth suppression or cell cycle arrest. Therefore, the effect of miR-944 on cell growth suppression may be dependent on p53 status.

As mentioned above, miR-944 in humans resides in an intron of p63 gene. Intronic microRNAs are generally transcribed together with their host genes [27]. For example, miR-106b, miR-93, and miR-25 reside in the intronic region of the MCM7 gene, which is involved in tumor progression in prostate cancer. The host gene (MCM7) and its intronic miRNAs are transcribed together after activation by the transcription factor c-myc. The intronic miRNA cluster targets the PTEN gene that suppresses MCM7 expression; as a result, the MCM7 function is maintained [28]. Another intronic microRNA, miR-301, has Ska2 as its host; miR-301 targets the 3′-UTR of MEOX2, resulting in an increase in transcription of Ska2, because MEOX2 is a negative regulator of Ska2 [29]. Unlike miR-301, miR-944 does not play a role in the transcriptional regulation of its host gene, p63, whereas the p63 protein activates the transcription of miR-944. Additionally, miR-944 has a promoter independent from the promoter of the host gene [11]. Although most intronic miRNAs share the promoter of their host genes [30], one third of them have their own promoters and transcription start sites [30]. In terms of evolution, younger miRNAs have mainly host-independent own promoter and transcription start site [31]. Therefore, it is not surprising that primate-specific miRNAs, including miR-944, have retained their own promoters and transcription start sites, as the phylogenetic group of primates is rather young in evolutionary terms.

In summary, in this study, we demonstrated that the miR-944, a primate-specific miRNA, is down-regulated in colorectal cancer cells and inhibits cell growth through cell cycle arrest. It exerts its tumor-suppressive function by targeting the ubiquitin ligases COP1 and MDM2, augmenting the tumor suppressor p53 signaling. These results suggest that miR-944 is an attractive drug target for cancer chemotherapy.

Conflicts of interest

The authors declare no conflict of interest.

Acknowledgement

This project was supported by grant from Basic Science Research Program through the National Research Foundation of Korea (NRF) (No. 2017R1A2B4009615).

Appendix A. Supplementary data

Supplementary data to this article can be found online at https://doi.org/10.1016/j.canlet.2018.10.029.

References

[1] J.J. Tjandra, M.K. Chan, Follow-up after curative resection of colorectal cancer: a meta-analysis, Dis. Colon Rectum 50 (2007) 1783–1799.
[2] T. Sjoblom, S. Jones, L.D. Wood, D.W. Parsons, J. Lin, T.D. Barber, et al., The consensus coding sequences of human breast and colorectal cancers, Science 314 (2006) 268–274.
[3] Y. Peng, C.M. Croce, The role of MicroRNAs in human cancer, Signal Transduct. Target. Ther. 1 (2016) 15004.
[4] G.A. Calin, C. Sevignani, C.D. Dumitru, T. Hyslop, E. Noch, S. Yendamuri, et al., Human microRNA genes are frequently located at fragile sites and genomic regions involved in cancers, Proc. Natl. Acad. Sci. U.S.A. 101 (2004) 2999–3004.
[5] J.F. Zhang, M.L. He, W.M. Fu, H. Wang, L.Z. Chen, X. Zhu, et al., Primate-specific microRNA-637 inhibits tumorigenesis in hepatocellular carcinoma by disrupting signal transducer and activator of transcription 3 signaling, Hepatology 54 (2011) 2137–2148.
[6] C. Perdomo, J.D. Campbell, J. Gerrein, C.S. Tellez, C.B. Garrison, T.C. Walser, et al., MicroRNA 4423 is a primate-specific regulator of airway epithelial cell differentiation and lung carcinogenesis, Proc. Natl. Acad. Sci. U.S.A. 110 (2013) 18946–18951.
[7] H. Suzuki, S. Takatsuka, H. Akashi, E. Yamamoto, M. Nojima, R. Maruyama, et al., Genome-wide profiling of chromatin signatures reveals epigenetic regulation of MicroRNA genes in colorectal cancer, Cancer Res. 71 (2011) 5646–5658.
[8] I. Nordentoft, K. Birkenkamp-Demtroder, M. Agerbæk, D. Theodorescu, M.S. Ostenfeld, A. Hartmann, et al., miRNAs associated with chemo-sensitivity in cell lines and in advanced bladder cancer, BMC Med. Genom. 5 (2012) 40.
[9] N.A. Schultz, K.K. Andersen, A. Roslind, H. Willenbrock, M. Wojdemann, J.S. Johansen, Prognostic microRNAs in cancer tissue from patients operated for pancreatic cancer-five microRNAs in a prognostic index, World J. Surg. 36 (2012) 2699–2707.
[10] T. Pan, W. Chen, X. Yuan, J. Shen, C. Qin, L. Wang, miR-944 inhibits metastasis of gastric cancer by preventing the epithelial-mesenchymal transition via MACC1/Met/AKT signaling, FEBS Open Bio 7 (2017) 905–914.
[11] K.H. Kim, E.G. Cho, S.J. Yu, H. Kang, Y.J. Kim, S.H. Kim, et al., DeltaNp63 intronic miR-944 is implicated in the DeltaNp63-mediated induction of epidermal differentiation, Nucleic Acids Res. 43 (2015) 7462–7479.
[12] U.A. Orom, A.H. Lund, Isolation of microRNA targets using biotinylated synthetic microRNAs, Methods 43 (2007) 162–165.
[13] Y. Hayashida, T. Nishibu, K. Inoue, T. Kurokawa, A useful approach to total analysis of RISC-associated RNA, BMC Res. Notes 2 (2009) 169.
[14] E. Li, P. Ji, N. Ouyang, Y. Zhang, X.Y. Wang, D.C. Rubin, et al., Differential expression of miRNAs in colon cancer between African and Caucasian Americans: implications for cancer racial health disparities, Int. J. Oncol. 45 (2014) 587–594.
[15] J. Sabates-Bellver, L.G. Van der Flier, M. de Palo, E. Cattaneo, C. Maake, H. Rehrauer, et al., Transcriptome profile of human colorectal adenomas, Mol. Canc. Res. 5 (2007) 1263–1275.
[16] L. Wen, Y. Li, Z. Jiang, Y. Zhang, B. Yang, F. Han, miR-944 inhibits cell migration and invasion by targeting MACC1 in colorectal cancer, Oncol. Rep. 37 (2017) 3415–3422.
[17] T. Soussi, B. Asselain, D. Hamroun, S. Kato, C. Ishioka, M. Claustres, et al., Meta-analysis of the p53 mutation database for mutant p53 biological activity reveals a methodologic bias in mutation detection, Clin. Canc. Res. 12 (2006) 62–69.
[18] Y. Hoffman, D.R. Bublik, Y. Pilpel, M. Oren, miR-661 downregulates both Mdm2 and Mdm4 to activate p53, Cell Death Differ. 21 (2014) 302–309.
[19] J. Zhang, Q. Sun, Z. Zhang, S. Ge, Z.G. Han, W.T. Chen, Loss of microRNA-143/145 disturbs cellular growth and apoptosis of human epithelial cancers by impairing the MDM2-p53 feedback loop, Oncogene 32 (2013) 61–69.
[20] F. Pichiorri, S.S. Suh, A. Rocci, L. De Luca, C. Taccioli, R. Santhanam, et al., Downregulation of p53-inducible microRNAs 192, 194, and 215 impairs the p53/MDM2 autoregulatory loop in multiple myeloma development, Cancer Cell 18 (2010) 367–381.
[21] M.D. Jansson, N.D. Damas, M. Lees, A. Jacobsen, A.H. Lund, miR-339-5p regulates the p53 tumor-suppressor pathway by targeting MDM2, Oncogene 34 (2015) 1908–1918.
[22] D. Dornan, I. Wertz, H. Shimizu, D. Arnott, G.D. Frantz, P. Dowd, et al., The ubiquitin ligase COP1 is a critical negative regulator of p53, Nature 429 (2004) 86–92.
[23] D. Dornan, H. Shimizu, A. Mah, T. Dudhela, M. Eby, K. O'rourke, et al., ATM engages autodegradation of the E3 ubiquitin ligase COP1 after DNA damage, Science 313 (2006) 1122–1126.
[24] H. Xie, L. Lee, P. Scicluna, E. Kavak, C. Larsson, R. Sandberg, et al., Novel functions and targets of miR-944 in human cervical cancer cells, Int. J. Canc. 136 (2015) E230–E241.
[25] J. Ma, K. Mannoor, L. Gao, A. Tan, M.A. Guarnera, M. Zhan, et al., Characterization of microRNA transcriptome in lung cancer by next-generation deep sequencing, Mol. Oncol. 8 (2014) 1208–1219.
[26] H. He, W. Tian, H. Chen, H. Huang, L.D. Hurst, J. Chen, MiR-944 functions as a novel oncogene and regulates the chemoresistance in breast cancer, Tumour Biology 37 (2016) 1599–1607.
[27] S. Baskerville, D.P. Bartel, Microarray profiling of microRNAs reveals frequent co-expression with neighboring miRNAs and host genes, RNA 11 (2015) 241–247.
[28] L. Poliseno, L. Salmena, L. Riccardi, A. Fornari, M.S. Song, R.M. Hobbs, et al., Identification of the miR-106b~25 microRNA cluster as a proto-oncogenic PTEN-targeting intron that cooperates with its host gene MCM7 in transformation, Sci.

Signal. 3 (2010) ra29.
[29] G. Cao, B. Huang, Z. Liu, J. Zhang, H. Xu, W. Xia, et al., Intronic miR-301 feedback regulates its host gene, ska2, in A549 cells by targeting MEOX2 to affect ERK/CREB pathways, Biochem. Biophys. Res. Commun. 396 (2010) 978–982.
[30] D. Lutter, C. Marr, J. Krumsiek, E.W. Lang, F.J. Theis, Intronic microRNAs support their host genes by mediating synergistic and antagonistic regulatory effects, BMC Genomics 11 (2010) 224.
[31] C. He, Z. Li, P. Chen, H. Huang, L.D. Hurst, J. Chen, Young intragenic miRNAs are less coexpressed with host genes than old ones: implications of miRNA-host gene coevolution, Nucleic Acids Res. 40 (2012) 4002–4012.